

DiscoSnp-RAD: de novo detection of small variants for RAD-Seq population genomics

Jérémy Gauthier¹, Charlotte Mouden¹, Tomasz Suchan², Nadir Alvarez³, Nils Arrigo³, Chloé Riou¹, Claire Lemaitre¹, Pierre Peterlongo^{Corresp. 1}

¹ Université de Rennes 1, Inria Rennes - Bretagne Atlantique, Rennes, France

² Institute of Botany, Polish Academy of Sciences, Krakow, Poland

³ Department of Ecology and Evolution, Université de Lausanne, Lausanne, Switzerland

Corresponding Author: Pierre Peterlongo
Email address: pierre.peterlongo@inria.fr

Restriction site Associated DNA Sequencing (RAD-Seq) is a technique characterized by the sequencing of specific loci along the genome, that is widely employed in the field of evolutionary biology since it allows to exploit variants (mainly Single Nucleotide Polymorphism - SNPs) information from entire populations at a reduced cost. Common RAD dedicated tools, such as STACKS or IPyRAD, are based on all-versus-all read alignments, which require consequent time and computing resources. We present an original method, DiscoSnp-RAD, that avoids this pitfall since variants are detected by exploring the De Bruijn Graph built from all the read datasets. We tested the implementation on simulated datasets of increasing size, up to 1000 samples, and on real RAD-Seq data from 259 specimens of *Chiastocheta* flies, morphologically assigned to 7 species. All individuals were successfully assigned to their species using both STRUCTURE and Maximum Likelihood phylogenetic reconstruction. Moreover, identified variants succeeded to reveal a within-species genetic structure and the existence of two populations linked to their geographic distributions. Furthermore, our results show that DiscoSnp-RAD is significantly faster than state-of-the-art tools. The overall results show that DiscoSnp-RAD is suitable to identify variants from RAD-Seq data, it does not require time-consuming parameterization steps and it stands out from other tools due to his completely different principle, making it substantially faster, in particular on large datasets.

License: GNU Affero general public license

Availability: DiscoSnp-RAD belongs to the DiscoSnp++ repository

<https://github.com/GATB/DiscoSnp/>

DiscoSnp-RAD: de novo detection of small variants for RAD-Seq population genomics

Jérémy Gauthier¹, Charlotte Mouden^{1,2}, Tomasz Suchan³, Nadir Alvarez^{4,5}, Nils Arrigo⁴, Chloé Riou¹, Claire Lemaitre¹, and Pierre Peterlongo¹

¹Univ Rennes, Inria, CNRS, IRISA, F-35000 Rennes, France

²INRA, BIOGECO, UMR1202, Cestas, France

³W. Szafer Institute of Botany, Polish Academy of Sciences, Kraków, Poland

⁴Department of Ecology and Evolution, University of Lausanne, Switzerland

⁵Natural History Museum of Geneva, Geneva, Switzerland

Corresponding author:

Pierre Peterlongo

Email address: pierre.peterlongo@inria.fr

ABSTRACT

Restriction site Associated DNA Sequencing (RAD-Seq) is a technique characterized by the sequencing of specific loci along the genome, that is widely employed in the field of evolutionary biology since it allows to exploit variants (mainly Single Nucleotide Polymorphism - SNPs) information from entire populations at a reduced cost. Common RAD dedicated tools, such as *STACKS* or *IPYRAD*, are based on all-versus-all read alignments, which require consequent time and computing resources. We present an original method, *DiscoSnp-RAD*, that avoids this pitfall since variants are detected by exploring the De Bruijn Graph built from all the read datasets. We tested the implementation on simulated datasets of increasing size, up to 1000 samples, and on real RAD-Seq data from 259 specimens of *Chiastocheta* flies, morphologically assigned to 7 species. All individuals were successfully assigned to their species using both STRUCTURE and Maximum Likelihood phylogenetic reconstruction. Moreover, identified variants succeeded to reveal a within-species genetic structure and the existence of two populations linked to their geographic distributions. Furthermore, our results show that *DiscoSnp-RAD* is significantly faster than state-of-the-art tools. The overall results show that *DiscoSnp-RAD* is suitable to identify variants from RAD-Seq data, it does not require time-consuming parameterization steps and it stands out from other tools due to his completely different principle, making it substantially faster, in particular on large datasets.

License: GNU Affero general public license

Availability: *DiscoSnp-RAD* belongs to the *DiscoSnp++* repository <https://github.com/GATB/DiscoSnp/>

1 INTRODUCTION

Next-generation sequencing and the ability to obtain genomic sequences for hundreds to thousands of individuals of the same species has opened new horizons in population genomics research. This has been made possible by the development of cost-efficient approaches to obtain sufficient homologous genomic regions, by reproducible genome complexity reduction and multiplexing several samples within a single sequencing run [1]. Among such methods, the most widely used over the last decade is “*Restriction-site Associated DNA sequencing*” (RAD-Seq). It uses restriction enzymes to digest DNA at specific genomic sites whose adjacent regions are then sequenced. This approach encompasses various methods with different intermediate steps to optimize the genome sampling, e.g. ddRAD [16], GBS [4], 2b-RAD [25], 3RAD/RADcap [9]. These methods share some basic steps: DNA digestion by one or more restriction enzymes, ligation of sequencing adapters and sample-specific barcodes, followed by optional fragmentation and fragment size selection, multiplexing samples bearing specific molecular tags, i.e.

47 indices and barcodes, and finally sequencing. The sequencing output is thus composed of hundreds of
48 thousands of reads originating from all the targeted homologous loci. The usual bioinformatic steps consist
49 in sample demultiplexing, clustering sequences in loci and identifying informative homologous variations.
50 If a reference genome exists, the most widely used strategy is to align the reads to this reference genome
51 and to perform a classical variant calling, focusing on small variants, Single Nucleotide Polymorphisms
52 (SNPs) and small Insertion-Deletions (INDELs). However, RAD-Seq approaches are mainly used on
53 non-model organisms for which a reference genome does not exist or is poorly assembled. The fact that
54 all reads sequenced from the same locus start and finish exactly at the same position makes it easy to
55 compare directly reads sequenced from a same locus. To *de novo* build homologous genomic loci and
56 extract informative variations, several methods have been developed, such as *STACKS* [2] and *PyRAD* [3],
57 as well as its derived rewritten version *IPyRAD* (<https://github.com/dereneaton/ipyrad>), being the most
58 commonly used in the population genomics community.

59 The main idea behind these approaches is to group reads by sequence similarity into clusters rep-
60 resenting each a distinct genomic locus. Since reads originating from the same locus start and end at
61 the same positions, they can be globally aligned, sequence variations can then be easily identified and a
62 consensus sequence is built for each locus. The key challenge is therefore the clustering part. To do so,
63 the classical approach relies on all-versus-all alignments. To reduce the number of alignments to compute,
64 the clustering is first performed within each sample independently, then sample consensus are compared
65 between samples. Nevertheless the number of alignments to perform remains very large and increases
66 quadratically with the number of reads. Importantly, analysis of RAD-Seq data is highly dependent on the
67 chosen clustering method, the sequencing quality and the dataset composition, such as the presence of inter
68 and/or intra-specific specimens or the number of individuals. Thus, existing tools allow customization of
69 numerous parameters to fine-tune the analysis. Particularly, both methods have parameters controlling the
70 granularity of clustering: the number of mismatches allowed between sequences of a same locus within
71 and among samples for *STACKS* and the percentage of similarity for *PyRAD*. These can be arbitrary fixed
72 by the user, but have a significant impact on downstream analyses [20].

73 We present here an utterly different approach to predict *de novo* small variants from large RAD-
74 Seq datasets, without performing any read clustering, avoiding all-versus-all read comparisons and
75 without relying on a critical similarity threshold parameter. It takes advantage of the *DiscoSnp++*
76 approach [24, 15], that was initially designed for *de novo* prediction of small variants, from shotgun
77 sequencing reads, without the need of a reference genome. The basic idea of the method is a careful
78 analysis of the *de Bruijn graph* built from all the input read sets, to identify topological motifs, often
79 called *bubbles*, generated by polymorphisms. In this work, we propose an adaptation of the *DiscoSnp++*
80 approach to the RAD-Seq data specificity. After validation tests on simulated datasets of increasing size,
81 we present an application of the *DiscoSnp-RAD* implementation on double-digest RAD-Seq data (ddRAD)
82 from a genus-wide sampling of parasitic flies belonging to *Chiastocheta* species. Using *DiscoSnp-RAD*,
83 the 259 individuals analyzed could be assigned to their respective species. Moreover, within-species
84 analyses focused on one of these species, identified variants revealing population structure congruent with
85 sample geographic origins. Thus, the information obtained from variants identified by *DiscoSnp-RAD*
86 can be successfully used for population genomic studies. The main notable difference between *DiscoSnp-RAD*
87 and concurrent algorithms stands in its easiness to use, without any parameter to test, and its execution
88 time, as it was substantially faster than *STACKS* run as well as *IPyRAD* run.

89 2 MATERIAL AND METHODS

90 2.1 *DiscoSnp-RAD*: RAD-Seq adaptation of *DiscoSnp++*

91 Originally, *DiscoSnp++* was designed for finding variants from whole genome sequencing data. To adapt
92 to the RAD-Seq context, the core algorithm of *DiscoSnp++* had to be extended and modified, as well as
93 the whole pipeline with particular post-processing.

94 ***DiscoSnp++* basic algorithm.** We first recall the fundamentals of the *DiscoSnp++* algorithm, which
95 is based on the analysis of the *de Bruijn Graph* (DBG) [17], which is a directed graph where the set
96 of vertices corresponds to the set of words of length k (k -mers) contained in the reads, and there is an
97 oriented edge between two k -mers, say s and t , if they perfectly overlap on $k - 1$ nucleotides, that is to say
98 if the last $k - 1$ suffix of s equals the first $k - 1$ prefix of t . In this case, we say that s can be *extended* by
99 the last character of t , thus forming a word of size $k + 1$. A node that has more than one predecessor and/or

more than one successor is called a branching node. Small variants, such as SNPs and INDELS, generate in the dBG recognizable patterns called “bubbles”. A bubble (Fig.1(a)) is defined by one *start* branching node that has, two distinct successor nodes. From these two children nodes, two paths exist and merge in a *stop* branching node, which has two predecessors. The type of the variant, whether it is a single isolated SNP, several close SNPs (distant from one another by less than k nucleotides) or an INDEL, determines the length of each of the two paths of the bubble.

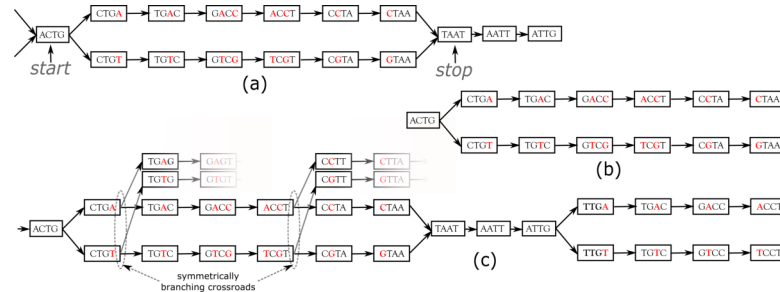


Figure 1. Examples of bubbles detected by SNPs in a toy de Bruijn graph, with $k = 4$. In (a) the bubble is complete: this corresponds to a bubble detected by *DiscoSnp++*. In (b), the bubble is symmetrically truncated: it is composed of a branching node (“ACTG”) whose two successors lead to two distinct paths that both have the same length and such that their last two nodes have no successor. Graph (c) shows an example of two bubbles from the same locus. The leftmost bubble contains two symmetrically crossroads.

DiscoSnp++ first builds a dBG from all the input read datasets combined, and then detects such bubbles. Sequencing errors or approximate repeats also generate such bubbles, that can be avoided by filtering out kmers with a too low abundance in the read sets, and by limiting the type or number of branching nodes along the two paths. Detected bubbles are output as pairs of sequences in fasta format. The second main step of *DiscoSnp++* consists in mapping original reads from all datasets on these sequences, in order to compute for each variant, read depth per allele and per read set. From this coverage information, genotypes are inferred and variants are scored. The final output is a VCF file, where each variant is associated to a confidence score (the *rank*) and is genotyped in each read set, thanks to its allele coverages (see [15, 24]).

In *DiscoSnp-RAD*, these two main steps have been modified to adapt to the RAD-seq context and an additional third step has been developed in order to cluster the variants per locus and to output this information in the final VCF file. In short, *DiscoSnp-RAD 1/* constructs the de Bruijn Graph and detects bubbles whose topology correspond to SNPs or indels, *2/* maps back reads on found bubble sequences, thus assessing the read coverage per allele and per read set, and *3/* performs clustering on predicted sequences. Those three steps are described in the three following sections.

2.1.1 Bubble detection with *DiscoSnp-RAD*

A novel RAD-specific bubble model. In *DiscoSnp++*, variants distant from less than k bp from a genomic extremity could not be detected, as associated bubbles do not open and/or close. This effect is negligible in the whole genome sequencing context, however, in the RAD-Seq context, sequenced genomic regions are limited to a hundred or to a few hundreds nucleotides (the read size), and thus a large amount of variants are likely to be located at the extremities of the loci. For instance, with reads of length 100bp, and $k = 31$ (which is a usual k value), on average 62% of the variants are located in the first or last k nucleotides of a locus and cannot be detected by *DiscoSnp++*.

In the RAD-Seq context, all reads sequenced from the same locus start and end exactly at the same position. Thus, variants located less than k bp from loci extremities generate what we call *Symmetrically Truncated Bubbles* (Fig.1(b)). Such bubbles start with a node which diverges into two distinct paths that do not meet back, such that both of them cannot be extended because of absence of successor and both paths have exactly the same length. Symmetrically, a variant located less than k bp apart from loci start generates a bubble that is right closed, but that starts with two unconnected paths of the same length.

To further increase specificity of the truncated bubble model, we also constrain the last 3-mer of both paths to be identical. Although this prevents the detection of variants as close as 3 bp from a locus extremity, this enables to identify correctly the type of detected variant. Indeed, when the last

138 L nucleotides of two locus sequences are different, several mutation events could have taken place in
 139 the genome resulting in the same observed differences: either an indel (of any size) or L successive
 140 substitutions or a combination of the two types. When L is small, all events may be equally parsimonious
 141 and we prefer to report none of these instead of a wrong one. This value was set to 3 because it leads to a
 142 relatively low loss of recall (6% with reads of length 100), while the probability of observing by chance
 143 three successive matches is low ($= \frac{1}{4^3} \approx 1.56\%$). Note that this issue is also present in any mapping or
 144 clustering based approaches.

145 The core of the *DiscoSnp-RAD* algorithm SNP bubble detection is sketched in Algorithm 1. Al-
 146 gorithm 1 is intentionally simplified and hides the process enabling to detect SNPs separated by less
 147 than k nucleotides and INDELS. The full and detailed algorithm is proposed in supplementary materials.
 148 Basically, after the graph construction, we loop over all its branching nodes (line 2), each branching
 149 node is then considered as a potential bubble extremity. The pair of paths that can be generated from
 150 this branching node are explored (lines 5 to the end). Notably, the two paths are created simultaneously
 151 nucleotide by nucleotide. The extension stops 1/ if the extension is impossible (line 10, if there exists no
 152 nucleotide α such that $kmer_1$ and $kmer_2$ can be extended with α); or 2/ if the bubble closes (line 11); or
 153 3/ if the bubble is truncated (line 7).

154 **Dealing with entangled bubbles.** As RAD-Seq data often include a large number of individuals, this
 155 is likely that many SNPs are close to each other (separated by less than k nucleotides), and that a large
 156 number of distinct haplotypes co-exist. This situation generates bubbles that are imbricated in one another
 157 and what we call “Symmetrically Branching Crossroads” (SBCs), as shown in Fig.1(c). SBCs appear
 158 when more than one unique character may be used during extension. By default, all possible extensions
 159 are explored (line 12) in presence of SBCs. We limit the maximal number of traversals of SBCs per bubble
 160 to 5 (line 14). This value has been chosen after tests showing that larger values lead to longer computation
 161 time, larger false positive calls (due to repetitive genomic regions), while not changing significantly recall
 162 results (data not shown). Depending on the user choice, we also propose a “high_precision” mode in
 163 which bubbles containing one or more SBC(s) are not detected.

Algorithm 1 Simplified overview of the *DiscoSnp-RAD* SNP bubble detection (Indel bubble detection omitted)

```

1: Create a de Bruijn Graph from all (any number  $\geq 1$ ) read set(s)
2: for Each right branching  $k$ -mer in the graph start do
3:   for each couple of successor  $kmer_1, kmer_2$  of  $k$ -mer start do
4:      $nb\_sym\_branching=0$ 
5:     while True do
6:       Extend  $kmer_1$  and  $kmer_2$  with  $\alpha \in \{A, C, G, T\}$ 
7:       if Both  $kmer_1$  and  $kmer_2$  have no successors then
8:         if last 3 characters from  $kmer_1$  and  $kmer_2$  are equal then
9:           Output bubble and break
10:        if Extension is impossible then break
11:        if  $kmer_1 = kmer_2$  then Output bubble and break
12:        if two or more possible extending nucleotides  $\alpha$  then
13:          Increase  $nb\_sym\_branching$ 
14:          if  $nb\_sym\_branching > 5$  then break
15:          else Explore recursively all possible extensions

```

164 2.1.2 Computing allele coverage and inferring genotypes

165 In this second step, original reads from all datasets are mapped on all bubble sequences, in order to
 166 provide the read coverage per allele and per read set. Importantly, this mapping step allows non-exact
 167 mapping, allowing up to 10 substitutions, except on the polymorphic positions of the bubble. These
 168 coverage information enables to infer individual genotypes and to assign a score (called *rank*) to each
 169 variant enabling to filter out potential false positive variants. Genotypes are inferred only if the sum of
 170 read counts for both alleles is above a *min_depth* threshold (by default 3), using a maximum likelihood
 171 strategy with a classical binomial model [15, 13], otherwise the genotype is indicated as missing (“./”).
 172 Variants with too many missing genotypes (more than 95 % of the samples) are filtered out.

173 Paralogous genomic regions represent a major issue in population genomic analyses as DNA sections
174 arising from duplication events can be aggregated in the same locus and thus, might encompass alleles not
175 deriving from coalescent events. Allele coverage information across many samples can be used to filter
176 out many of such paralog-induced variants. As approximated repeats tend to occur in all the samples,
177 their allele frequency is thus non discriminant between samples. An efficient scoring scheme, called the
178 *rank* value in *DiscoSnp++*, reflects such discriminant power of variants. This is defined as the maximal
179 Phi coefficient of allele read counts contingency table over all possible pairs of datasets, with one Phi
180 coefficient being computed as follows: $\sqrt{\frac{\chi^2}{n}}$, with n being the sum of read counts for this pair of datasets.
181 We have shown in previous work [24, 15] that approximate repeats are likely to generate bubbles in the
182 dBG but with very low rank values (< 0.4) contrary to real variants. This filter is particularly effective
183 when many samples are compared, as in the RAD-seq context. Thus, by default, *DiscoSnp-RAD* discards
184 all variants with such low rank values.

185 **2.1.3 Clustering variants per loci**

186 During the bubble detection phase, several independent bubbles can be predicted for the same RAD
187 locus. For instance, Fig.1(c) shows a toy example of a the dBG graph associated to a locus. In this
188 case, *DiscoSnp-RAD* detects two bubbles, that give no sign of physical proximity. In several population
189 genomics analyses, such proximity information can be useful, such as in population structure analyses,
190 where this is recommended to select only one variant per locus. In order to recover this information of
191 locus membership, we developed a post-processing method to cluster predicted variants per locus.

192 The method uses the fact that *DiscoSnp-RAD* is parameterized to output bubbles together with their left
193 and right contexts in the graph, which correspond to the paths starting from each extreme node and ending
194 at the first ambiguity (ie. a node with not exactly one successor). In this case, the two bubbles of Fig.1
195 are output as 2x2 longer sequences (ACTG**A**CCTAATTG/ACTG**T**CGTAATTG and TAATTG**A**CCT/
196 TAATTG**T**CCT) that share at least one $k - 1$ -mer (here $k - 1$ -mers TAA, AAT, ATT and TTG).

197 If a given locus contains several variants, each bubble of this locus should share one $k - 1$ -mer with
198 at least one other bubble of the same locus. We exploit this property to group all bubbles per locus. For
199 doing so, we create a graph in which a node is a bubble (represented by its pair of sequences), and there is
200 an edge between two nodes if the corresponding sequences share at least one $k - 1$ -mer. This is done using
201 *SRC_linker* [12]. Finally, we partition this graph by connected component. Each connected component
202 contains all bubbles for a given locus and this information is reported in the vcf file. Clusters containing
203 more than 150 variants are discarded, as they are likely to aggregate paralogous variants from repetitive
204 regions.

205 **2.1.4 Various optional filtering options**

206 The output of *DiscoSnp-RAD* is a VCF file containing predicted variants along with various information,
207 such as their genotypes and allele read counts in all samples, their *rank* value and the cluster ID (locus)
208 they belong to. This enables to apply custom filters at the locus level, as well as any variant level
209 classical RAD-Seq filters (such as the minimal read depth to call a genotype or the minimal minor
210 allele frequency to keep a variant). Several such RAD-seq filtering scripts are provided along with
211 the main program ([https://github.com/GATB/DiscoSnp/tree/master/discoSnpRAD/
212 post-processing_scripts](https://github.com/GATB/DiscoSnp/tree/master/discoSnpRAD/post-processing_scripts)).

213 **2.2 Testing environment**

214 The tests were performed on the GenOuest (genouest.org) cluster, on a node composed of 40 Intel
215 Xeon core processors with speed 2.6 GHz and 252 GB of RAM.

216 **2.3 Validation on simulated datasets**

217 **Simulation protocol.** RAD loci from *Drosophila melanogaster* genome (dm6) were simulated by
218 selecting 150 bp on both sides of 43,848 PstI restriction sites resulting in 87,696 loci. Several populations,
219 each composed of several diploid individuals were simulated as follows. For each simulated population,
220 SNPs were randomly generated at a rate of 0.01%. A first subset of them (70%) was introduced in all
221 samples from the population and represent shared polymorphism. The rest of these SNPs (30%) were
222 distributed between samples by a random picking of 10% of them and assigned to each sample. For
223 each sample, 10% of the assigned SNPs, shared and sample specific, are introduced in only one of the
224 homologous chromosomes to simulate heterozygosity. This process was repeated to generate from 5 to 50

225 populations each composed of 20 individuals. Finally, between 2,109,900 SNPs for 100 samples, and
226 2,547,337 SNPs for 1,000 samples, were generated. Forward 150bp reads were simulated on right and
227 left loci, with 1% sequencing errors, with 20X coverage per individual (the complete pipeline is given in
228 Supplementary Figure 1).

229 **Evaluation protocol.** For estimating the result quality, predicted variants were localized on the *D.*
230 *melanogaster* genome and output in a vcf file. To do so, we used the standard protocol of *DiscoSnp++*
231 when a reference genome is provided, using BWA-mem [11]. The predicted vcf was compared to the
232 vcf storing simulated variant positions to compute the amount of common variants (true positive or TP),
233 predicted but not simulated variants (false positive or FP) and simulated but not predicted variants (false
234 negative or FN). Recall is then defined as $\frac{\#TP}{\#TP+\#FN}$, and precision as $\frac{\#TP}{\#TP+\#FP}$.

235 **Comparison with other tools.** For comparisons, *STACKS* v2.4 and *IPyRAD* v0.7.30 were run on the
236 simulated datasets. *STACKS* stacks were generated *de novo* (`denovo_map.pl`), with a minimum of 3
237 reads to consider a stack (`-m 3`). On the simulated dataset composed of 100 samples, five values of the
238 parameter `-M` governing stack merging (ie. 4, 6, 8, 10, and 12) were tested. On the remaining datasets,
239 the parameter `-M` was fixed to 6. All other parameters were set to default values. Similarly, *IPyRAD* was
240 run using five values of clustering threshold on the dataset composed of 100 samples (ie.) and then fixed
241 to 0.80 for larger datasets. The other parameters have been kept at the default values.

242 Then, *de novo* tags from *STACKS* and loci from *IPyRAD* were mapped to the *D. melanogaster* genome.
243 For *STACKS*, loci were mapped using GSNAP/GMAP [26]. Genomic coordinates were incorporated
244 in outputs using a script provided in the *STACKS* tools suite, before generating a vcf file with the
245 `populations` module [14]. For *IPyRAD*, loci were mapped to the *D. melanogaster* genome using
246 BWA-mem and variant positions were transposed on the genome positions with a custom script.

247 2.4 Application to real data from *Chiastocheta* species

248 **Data origin.** Tests on real data were performed on ddRAD reads previously obtained for the phylogenetic
249 study of seed parasitic pollinators from the genus *Chiastocheta* (Diptera: Anthomyiidae). The dataset
250 corresponds to the sequencing of 259 individuals sampled from 51 European localities generated by
251 Lausanne University, Switzerland [22] (<https://www.ebi.ac.uk/ena/data/view/PRJEB23593>). A total of
252 608,367,380 reads were used for the study with an average of 2.3 Million reads per individual.

253 **Variant prediction and filtering.** *DiscoSnp-RAD* was run with default parameters, searching for at most
254 five variants per bubble. Downstream classical filters were applied to follow as much as possible the filters
255 used in the Suchan *et al.* study [22]: a minimum genotype coverage of 6, a minimal minor allele frequency
256 of 0.01 and a minimum of 60% of the samples with a non missing genotype for each variant. These filters
257 remove less informative variants or those with an allele specific to a very small subset of samples. These
258 filters were also applied at the intra-specific level in one of the seven sampled *Chiastocheta* species, i.e. *C.*
259 *lophota*, on the same *DiscoSnp++* output.

260 **Population genomic analyses.** The species genetic structure was inferred using STRUCTURE [18]
261 v2.3.4. This approach requires unlinked markers, thus only one variant by locus, randomly selected, has
262 been kept. The STRUCTURE analysis was carried on the datasets generated by each tool. Simulations
263 were performed with genetic cluster number (*K*) set to 7, corresponding to the seven species described
264 in [22]. We used 20,000 MCMC iterations after a burn-in period of 10,000. The output is the posterior
265 probability of each sample to belong to each of the seven possible clusters.

266 **Phylogenomic analyses.** Maximum likelihood (ML) phylogenetic reconstruction was performed
267 on a whole concatenated SNP dataset using GTRGAMMA model with the acquisition bias correc-
268 tion [10]. We applied rapid Bootstrap analysis with the extended majority-rule consensus tree stopping
269 criterion and search for best-scoring ML tree in one run, followed by ML search, as implemented in
270 RAxML v8.2.11 [21].

271 3 RESULTS

272 3.1 Results on simulated data

273 *DiscoSnp-RAD* was first run on several simulated RAD-Seq datasets composed of an increasing number of
274 samples (from 100 to 1,000) in order to validate the approach, to evaluate its speed and efficiency and to

275 compare it with the other clustering approaches. This experiment shows that *DiscoSnp-RAD* predictions
 276 are accurate with a good compromise between recall and precision (see Figure 2). On average, 84.6 % of
 277 the simulated variants are recovered with very few false positive calls, ie. reaching a precision of 98.5
 278 % on average. Importantly, these performances are not impacted by the number of input samples in the
 279 dataset. For instance, recall varies from 84.6% to 83.3% between the smallest and the largest datasets (100
 280 vs 1.000 samples), and precision from 98.1 % to 98.5%. By comparison with other tools, for each of the
 281 tested population sizes, recall and precision are comparable between tools, with typically a recall lower
 282 than *STACKS* and *IPyRAD* and an intermediate precision, lower than *IPyRAD* and higher than *STACKS*.
 283 The loss of recall may be explained by the fact that *DiscoSnp-RAD* voluntarily does not detect the variants
 284 within 3 bp of each locus end (see Methods). The main differences between the tools concern the run
 285 time and the disk space usage. These differences increase with the number of samples in the dataset. For
 286 instance, on the largest dataset composed of 1,000 samples *DiscoSnp-RAD* is more than 3 times faster
 287 than *STACKS* and more than 5 times faster than *IPyRAD*. Moreover, if we consider the cumulative time
 288 required to test different parameters for *STACKS* and *IPyRAD*, i.e. five sets of parameters for each tool,
 289 *DiscoSnp-RAD*, without parameter setting is more than 15 times faster than *STACKS* and more than 25
 290 times faster than *IPyRAD*. Regarding the disk space used by the tool during the process, *DiscoSnp-RAD*
 291 requires only a small amount of space compared to the other tools. Full RAM memory, disk usage, and
 292 computation times of *DiscoSnp-RAD* are provided in Supplementary Table 1.

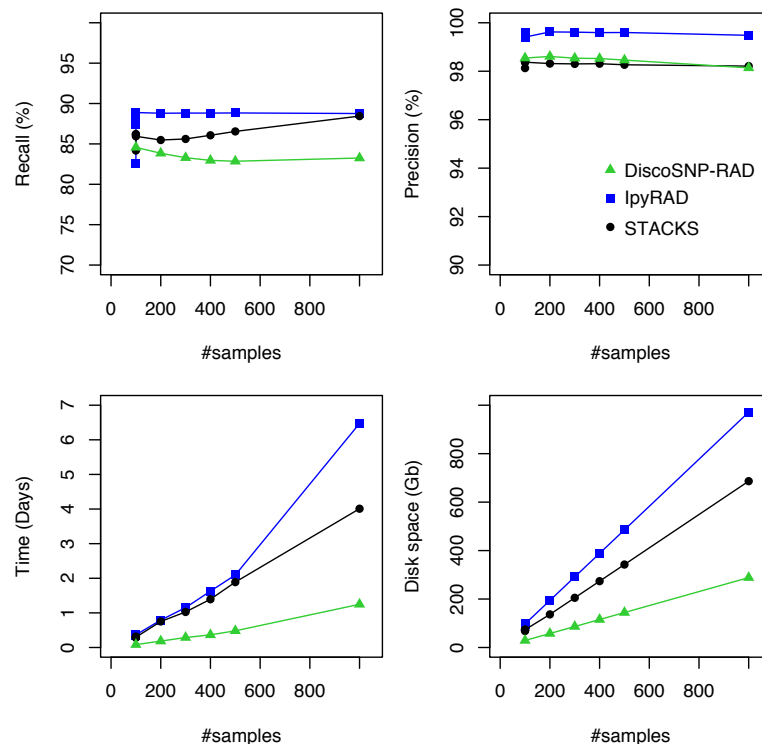


Figure 2. Recall, precision, time and space evolution on simulated data with different sampling sizes. For the sampling of 100 samples, five parameter sets were tested for *IPyRAD* and *STACKS* (see Material and Methods for details).

293 **Robustness with respect to parameters.** A major advantage of *DiscoSnp-RAD* stands in the fact that
 294 it does not require fine parameter tuning. This is an important point as other state-of-the-art tools are
 295 extremely sensible to their parameters, especially those directly linked to the expected sequence divergence
 296 between samples, and require time consuming processes to set them properly [20]. In *DiscoSnp-RAD*, the
 297 main parameter is the size of k -mers, used for building the dBG. As shown Figure 3, *DiscoSnp-RAD*
 298 results are robust with respect to k , and its fine choice is thus not crucial.

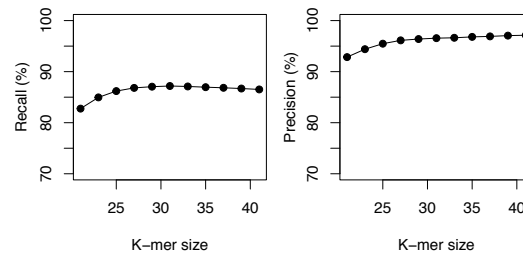


Figure 3. Recall and precision on simulated data of 100 samples using DiscoSnp-RAD and different K-mer sizes from 21 to 41.

299 3.2 Results on real data

300 In this section, we present an application of the *DiscoSnp-RAD* implementation on ddRAD sequences
 301 obtained from the anthomyiid flies from the *Chiastocheta* genus. In this genus, classical mitochondrial
 302 markers are not suitable for discriminating the morphologically described species [5]. Although RAD-
 303 sequencing dataset phylogenies supported the species assignment [22], the interspecific relationships
 304 between the taxa could not be resolved with high confidence due to high levels of incongruences in gene
 305 trees [7, 22]. The dataset is composed of 259 sequenced individuals from 7 species. Results obtained on
 306 *DiscoSnp-RAD* were compared to the prior work of Suchan and colleagues, based on *pyRAD* analysis [22].
 307 In addition, we provide a performance benchmark of *STACKS*, *IPyRAD* and *DiscoSnp-RAD* run on this
 308 dataset.

309 **Recovering all *Chiastocheta* species.** Variant calling was run on the 259 *Chiastocheta* samples with
 310 *DiscoSnp-RAD*. Before filtering, 115,920 SNPs were identified. After filtering, 4,364 SNPs, located in
 311 1,970 clusters, were retained and used for population genomic analyses. The total number of clusters is
 312 coherent with the 1,672 loci from Suchan *et al.* [22].

313 Then, following the requirements of the STRUCTURE algorithm, only one variant per cluster was
 314 retained, resulting in a dataset composed of 1,970 SNPs. STRUCTURE successfully assigned samples
 315 to the seven species, consistent with the morphological species assignment and previously published
 316 results [22] (Fig.4). The assignment values represent the probability with which STRUCTURE assigns a
 317 sample to a cluster, depending on the information carried by the variants. Theoretically and in an extreme
 318 case, if all variants of a sample are completely differentiated, different from the others and specific to a
 319 cluster or species, the assignment will be 1. The assignment values are high with an average of 0.992
 320 (sd 0.022) across samples and a minimum assignment of 0.810. These values are comparable to the
 321 assignment values obtained by Suchan *et al.* [22] with an average of 0.977 (sd 0.042) and a minimum of
 322 0.685. Genetic structure has also been investigated for the two other tools and give very similar population
 323 assignments (Supplementary Figure 2).

324 The phylogeny realized with RAxML on the 4,364 SNPs obtained after filtering, is congruent with the
 325 one obtained by Suchan and colleagues [22] (Fig.4). The internal branches separating the seven species
 326 are well supported by high bootstrap values.

327 **Recovering phylogeographic patterns.** To assess the utility of *DiscoSnp-RAD* dataset for investigating
 328 the intra-specific genetic structure, we then focused the analysis on 40 samples of *C. lophota* species. The
 329 same run of *DiscoSnp-RAD* obtained with the 259 samples was used, only the vcf was limited to the 40
 330 sample columns of this species and the same filters were applied on this reduced dataset. We obtained
 331 1,306 SNPs by selecting one variant per locus extracted from 4,364 variants identified in this species. The
 332 STRUCTURE analysis of this dataset tended to identify two populations and assigned 31 samples to one
 333 of them and 9 to the other (Fig.4). Notably, the genetic structure follows the geographic distribution of
 334 the samples, with samples assigned to one population originating from western locations as opposed to
 335 samples assigned to the second population. Geographic structuring is the most frequent structuration
 336 factor observed in population genetics, pointing to the geographical isolation of divergent lineages. This
 337 clear geographic structuring is another hint that *DiscoSnp-RAD* recovers real biogeographic signal.

338 **Breakthrough in running time.** *DiscoSnp-RAD* run on the 259 *Chiastocheta* samples took about 30
 339 hours. This comprises the whole process from building the DBG to obtaining the final filtered vcf file with

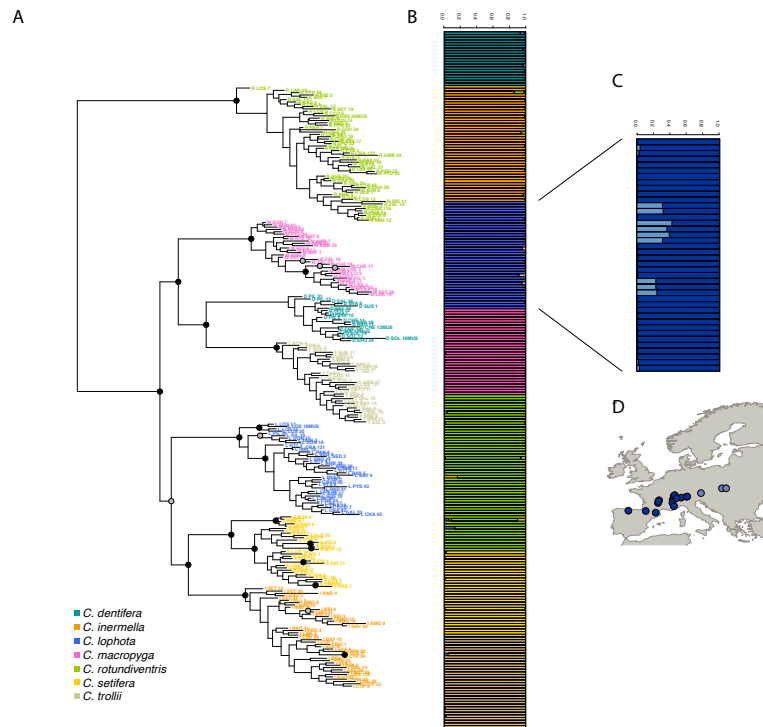


Figure 4. a. RAxML phylogeny realized on all variants predicted by *DiscoSnp-RAD*. Bootstrap node supports > 80 are shown denoted by gray dots, bootstrap node supports > 90 are shown denoted by black dots. b. STRUCTURE results obtained with SNP only and all variants on the seven *Chiastocheta* species. c. *C. lophota* sample genetic structure and their geographic distribution.

340 for instance 1 SNP per locus. To compare the *DiscoSnp-RAD* performances with *STACKS* and *IPyRAD*
 341 on real data, we ran each of these tools using default parameters on the 259 *Chiastocheta* samples and
 342 measured running time and maximum memory usage. The difference is remarkable, *DiscoSnp-RAD* is
 343 more than 4.65 times faster than *STACKS* (running time 138 hours) and 2.8 times faster than *IPyRAD*
 344 (running time 82 hours) to perform the whole process. Moreover, contrary to *DiscoSnp-RAD*, *STACKS*
 345 and *IPyRAD* should be run several times to explore the parameters which represent a considerable amount
 346 of time and memory. For instance, in Suchan *et al.* [22], *IPyRAD* was run with 5 different combinations
 347 of parameter values, *DiscoSnp-RAD* being thus 14 times faster than *IPyRAD*.

348 4 DISCUSSION

349 ***DiscoSnp-RAD* efficiency.** *DiscoSnp-RAD* produced relevant results on ddRAD data from *Chiastocheta*
 350 species. SNPs identified allowed us to successfully i) distinguish the seven species based on the STRUC-
 351 TURE algorithm, and ii) reconstruct the phylogenetic tree of the genus, congruent with the previously
 352 published one [22]. Moreover, on the intraspecific scale, we obtained geographically meaningful results
 353 within *C. lophota* species. The variants identified by *DiscoSnp-RAD* can be used to study the species or
 354 population genetic structure and could be used to investigate deeper the mechanisms at the origin of this
 355 structure such as potential gene flow between populations or their demographic histories. In addition,
 356 *DiscoSnp-RAD* is also able to identify INDELS [15], they were not used in this study but are available
 357 for users. Furthermore, the use of *DiscoSnp-RAD* presented considerable advantages in the run-time, and
 358 parameters choice, compared to other common *de novo* RAD analysis tools, as described below.

359 **Run-time.** The use of *DiscoSnp-RAD* dramatically decreased the overall time for discovering and
 360 selecting relevant variants, as compared to other tools. Moreover, *DiscoSnp-RAD* speed is less dependant
 361 on the number of reads and is not expected to increase quadratically with dataset size, as it is the case
 362 for pair-wise alignment based tools such as *STACKS* and *PyRAD*. This can likely be anticipated that

363 with the drop of sequencing costs, RAD projects will grow in size, either by using higher frequency
364 cutting enzymes to obtain a dense genome screening, by increasing the sequencing depth to compensate
365 sequencing variation or by increasing the number of samples. In this context, *DiscoSnp-RAD* will more
366 easily scale to such very large datasets.

367 **Easy parameter choice.** Another substantial advantage of using *DiscoSnp-RAD* is the fact that param-
368 eters are not directly linked to the level of expected divergence of the compared samples. In fact, they
369 impact the number and type of detected variants, but are not related to the subsequent clustering step. As
370 a result, same parameters can be used whatever the type of analysis (for example, intra or inter-specific),
371 contrasting with classical tools in which parameters govern loci recovering. Indeed, in *STACKS*, the
372 parameters governing the merge of the stacks can compromise the detection of relevant variants if they are
373 not adapted to the studied dataset [20]. Therefore, the authors recommend to perform an exploration of
374 the parameter space before downstream analyses [14]. This is extremely time consuming, up to one month
375 as confessed by the authors [19], and may not always result in interpretable conclusions. In *IPyRAD*, the
376 similarity parameter for clustering also impacts variant detection, and usually several values have to be
377 tested to choose the best, as exemplified by Suchan and colleagues who tested five different values [22].

378 **By-locus assembly.** *DiscoSnp-RAD* output is a vcf file including pseudo-loci information, that allows
379 the application of standard variant filtering pipelines. One next objective is to recover loci consensus
380 sequences, that could be used for phylogenetic analysis based on full locus sequences. This could be
381 achieved by performing local assemblies per individual, from all bubbles contained in a cluster.

382 **Potential applications.** In many RAD-Seq studies using paired-end sequencing, the second read, i.e.
383 one half of the sequencing effort, is mainly used to remove PCR duplicates and rarely exploited to detect
384 variants. Indeed, in such cases, reads 2 do not start and finish at the same position. Properly recovery
385 of loci is therefore not possible with read stacking approaches. This problem does not exist when using
386 *DiscoSnp-RAD*, and variants present in reads 2 can also be called. Indeed, the *DiscoSnp-RAD* method,
387 being not based on stacks of reads, is able to detect any variants that generate bubble motifs in the DBG,
388 thus even if present in reads whose starting positions differ.

389 This ability of *DiscoSnp-RAD* to handle reads that do not necessary start at the same genomic position
390 makes it particularly well suited to analyze the datasets produced by another group of genome-reduction
391 techniques, namely sequence capture approaches [8]. In these techniques, DNA shotgun libraries are
392 subject to enrichment using short commercially-synthesized [6] or in-house made [23] DNA or RNA
393 fragments acting as 'molecular baits', that hybridize and allow separation of homologous fragments
394 from genomic libraries. One of such promising approaches is HyRAD, a RAD approach combining
395 the molecular probes generated using ddRAD technique and targeted capture sequencing, designed for
396 studying old and/or poor quality DNA, likely to be too fragmented for RAD-sequencing [23]. In HyRAD,
397 capturing randomly fragmented DNA results in reads not strictly aligned and covering larger genomic
398 regions than RAD-Seq. Therefore RAD tools can not be used to reconstruct such loci, and the current
399 analysis consists in building loci consensuses from reads, and then calling variants by mapping back the
400 reads on it. The use of *DiscoSnp-RAD* should simplify this process in a single *de novo* calling step.

401 ACKNOWLEDGMENTS

402 Authors thank Camille Marchet for her precious help on the clustering implementation. Computations
403 have been made possible thanks to the resources of the Genouest infrastructures. This work was supported
404 by the French ANR-14-CE02-0011 SPECREP grant.

405 REFERENCES

- 406 [1] Andrews, K., Good, J., R Miller, M., Luikart, G., and A Hohenlohe, P. (2016). Harnessing the power
407 of radseq for ecological and evolutionary genomics. *Nature Reviews Genetics*, 17:81–92.
- 408 [2] Catchen, J., Hohenlohe, P. A., Bassham, S., Amores, A., and Cresko, W. A. (2013). Stacks: an analysis
409 tool set for population genomics. *Molecular Ecology*, 22(11):3124–3140.
- 410 [3] Eaton, D. A. R. (2014). Pyrad: assembly of de novo radseq loci for phylogenetic analyses. *Bioinform-*
411 *atics*, 30(13):1844–1849.

- 412 [4] Elshire, R. J., Glaubitz, J. C., Sun, Q., Poland, J. A., Kawamoto, K., Buckler, E. S., and Mitchell, S. E.
413 (2011). A robust, simple genotyping-by-sequencing (gbs) approach for high diversity species. *PLOS*
414 *ONE*, 6(5):1–10.
- 415 [5] Espíndola, A., Buerki, S., and Alvarez, N. (2012). Ecological and historical drivers of diversification
416 in the fly genus *Chiaetocheta pokorny*. *Molecular Phylogenetics and Evolution*, 63(2):466–474.
- 417 [6] Faircloth, B. C., McCormack, J. E., Crawford, N. G., Harvey, M. G., Brumfield, R. T., and Glenn, T. C.
418 (2012). Ultraconserved elements anchor thousands of genetic markers spanning multiple evolutionary
419 timescales. *Systematic Biology*, 61(5):717–726.
- 420 [7] Gori, K., Suchan, T., Alvarez, N., Goldman, N., and Dessimoz, C. (2016). Clustering genes of
421 common evolutionary history. *Molecular Biology and Evolution*, 33(6):1590–1605.
- 422 [8] Grover, C. E., Salmon, A., and Wendel, J. F. (2012). Targeted sequence capture as a powerful tool for
423 evolutionary analysis. *American Journal of Botany*, 99(2):312–319.
- 424 [9] Hoffberg, S. L., Kieran, T. J., Catchen, J. M., Devault, A., Faircloth, B. C., Mauricio, R., and Glenn,
425 T. C. (2016). Radcap: sequence capture of dual-digest radseq libraries with identifiable duplicates and
426 reduced missing data. *Molecular Ecology Resources*, 16(5):1264–1278.
- 427 [10] Leaché, A. D., Banbury, B. L., Felsenstein, J., de Oca, A. N.-M., and Stamatakis, A. (2015). Short
428 tree, long tree, right tree, wrong tree: new acquisition bias corrections for inferring snp phylogenies.
429 *Systematic Biology*, 64(6):1032–1047.
- 430 [11] Li, H. and Durbin, R. (2009). Fast and accurate short read alignment with Burrows-Wheeler transform.
431 *Bioinformatics*, 25(14):1754–1760.
- 432 [12] Marchet, C., Limasset, A., Bittner, L., and Peterlongo, P. (2016). A resource-frugal probabilistic
433 dictionary and applications in (meta)genomics. *CoRR*, abs/1605.08319.
- 434 [13] Nielsen, R., Paul, J. S., Albrechtsen, A., and Song, Y. S. (2011). Genotype and SNP calling from
435 next-generation sequencing data. *Nature Reviews Genetics*, 12:443–451.
- 436 [14] Paris, J. R., Stevens, J. R., and Catchen, J. M. (2017). Lost in parameter space: a road map for stacks.
437 *Methods in Ecology and Evolution*, 8(10):1360–1373.
- 438 [15] Peterlongo, P., Riou, C., Drezen, E., and Lemaitre, C. (2017). Discosnp++: de novo detection of
439 small variants from raw unassembled read set(s). *bioRxiv*.
- 440 [16] Peterson, B. K., Weber, J. N., Kay, E. H., Fisher, H. S., and Hoekstra, H. E. (2012). Double digest
441 radseq: An inexpensive method for de novo snp discovery and genotyping in model and non-model
442 species. *PLOS ONE*, 7(5):1–11.
- 443 [17] Pevzner, P. A., Tang, H., and Tesler, G. (2004). De novo repeat classification and fragment assembly.
444 *Genome Research*, 14(9):1786–1796.
- 445 [18] Pritchard, J. K., Stephens, M., and Donnelly, P. (2000). Inference of population structure using
446 multilocus genotype data. *Genetics*, 155(2):945–959.
- 447 [19] Rochette, N. C. and Catchen, J. M. (2017). Deriving genotypes from RAD-seq short-read data using
448 Stacks. *Nature Protocols*, 12(12):2640–2659.
- 449 [20] Shafer, A. B. A., Peart, C. R., Tusso, S., Maayan, I., Brelsford, A., Wheat, C. W., and Wolf, J. B. W.
450 (2017). Bioinformatic processing of rad-seq data dramatically impacts downstream population genetic
451 inference. *Methods in Ecology and Evolution*, 8(8):907–917.
- 452 [21] Stamatakis, A. (2014). Raxml version 8: a tool for phylogenetic analysis and post-analysis of large
453 phylogenies. *Bioinformatics*, 30(9):1312–1313.
- 454 [22] Suchan, T., Espíndola, A., Rutschmann, S., Emerson, B. C., Gori, K., Dessimoz, C., Arrigo, N.,
455 Ronikier, M., and Alvarez, N. (2017). Assessing the potential of rad-sequencing to resolve phylogenetic
456 relationships within species radiations: The fly genus *Chiaetocheta* (Diptera: Anthomyiidae) as a case
457 study. *Molecular Phylogenetics and Evolution*, 114:189–198.
- 458 [23] Suchan, T., Pitteloud, C., Gerasimova, N. S., Kostikova, A., Schmid, S., Arrigo, N., Pajkovic, M.,
459 Ronikier, M., and Alvarez, N. (2016). Hybridization capture using rad probes (hyrad), a new tool for
460 performing genomic analyses on collection specimens. *PLOS ONE*, 11(3):1–22.
- 461 [24] Uricaru, R., Rizk, G., Lacroix, V., Quillery, E., Plantard, O., Chikhi, R., Lemaitre, C., and Peterlongo,
462 P. (2014). Reference-free detection of isolated SNPs. *Nucleic Acids Research*, 43(2):1–11.
- 463 [25] Wang, S., Meyer, E., McKay, J., and Matz, M. (2012). 2b-rad: A simple and flexible method for
464 genome-wide genotyping. *Nature Methods*, 9:808–810.
- 465 [26] Wu, T. D. and Nacu, S. (2010). Fast and snp-tolerant detection of complex variants and splicing in
466 short reads. *Bioinformatics*, 26(7):873–881.